Morphology-dependent resonances in an eccentrically layered sphere illuminated by a tightly focused off-axis Gaussian beam: parallel and perpendicular beam incidence

J. J. Wang,[1,2,*] G. Gouesbet,[1] G. Gréhan,[1] Y. P. Han,[2] and S. Saengkaew[1]

[1]*Laboratoire d'Electromagnétisme des Systèmes Particulaires (LESP), Unité Mixte de Recherche (UMR) 6614 du Centre National de la Recherche Scientifique (CNRS), COmplexe de Recherche Interprofessionnel en Aérothermochimie (CORIA), Université de Rouen, et Institut National des Sciences Appliquées (INSA) de Rouen, BP12, avenue de l'université, technopôle du Madrillet, 76801 Saint-Etienne-du Rouvray, France*

[2]*School of Science, Xidian University, 710071 Xi'an, China*

**Corresponding author: jiajie.wang@coria.fr*

Received May 24, 2011; accepted July 13, 2011;
posted July 18, 2011 (Doc. ID 148104); published August 22, 2011

Following the recent results in generalized Lorenz–Mie theory concerning the description of an arbitrary shaped electromagnetic beam propagating in an arbitrary orientation, a theoretical investigation of morphology-dependent resonances (MDRs) excited in a sphere with an eccentrically located spherical inclusion illuminated by a tightly focused Gaussian beam is presented. Calculations of extinction efficiency spectra and backward-scattering intensity spectra are made for different locations and radii of the inclusion with respect to the host sphere. Exemplifying field distributions inside of the scatterer under both off-resonance and on-resonance conditions are exhibited. The influences of the relative size of the inclusion with respect to the host sphere and of the separation distance between the two sphere centers on the positions and on the amplitudes of the MDRs peaks are studied. As are the cases for spheres and concentrically multilayered spheres, the resonance positions of MDRs in an eccentrically layered sphere are located at the same size parameter for Gaussian beam illumination and for plane-wave illumination. In contrast with the lift of azimuthal modes m degeneracy in MDR peaks for an eccentric sphere illuminated obliquely by a plane wave, we display a kind of lift that cannot be observed in extinction efficiency spectra with an oblique illumination of a tightly focused Gaussian beam. Nevertheless, asymmetric distributions of the internal field inside of the eccentric sphere at resonance conditions are observed both with an oblique illumination of a tightly focused beam and with an oblique illumination of a plane-wave illumination. Interpretation from a perspective of the localization principle is applied to the simulation results.

OCIS codes: 260.2110, 140.3430.

1. INTRODUCTION

Morphology-dependent resonances (MDRs) generated by a spherical surface are believed to be first described by Lord Rayleigh a century ago, but only after the invention of laser did they start to have more scientific relevance, and it is only during the past three decades that there has been a substantial move toward extensive practical applications. MDRs were first observed in radiation pressure experiments on dielectric spheres while levitating a droplet by a tightly focused laser beam [1]. Numerical simulations carried out with high resolution by using the Mie–Debye theory were given very soon after [2], and remarkable agreement with the experimental observations of MDRs was shown. Because of the fact that the positions and the widths of MDRs are highly sensitive to the size parameter and to the refractive index of the scatterers (in particular droplets), MDR-related optical techniques, based on the properties of MDR peaks in elastic scattering spectra [3] or in inelastic scattering spectra [4], were introduced to detect various properties of droplets. With extensive investigations in the past decades [5,6], a reliable optical tool for optical particle characterization is now available. Relying on the precise measurement of the positions and of the widths of the MDR peaks by high-resolution spectroscopy, absolute sizes of spheres can be obtained to a precision of 1 part in 10^5. By measuring the wavelength shift of MDR peaks in the scattering spectrum, evaporation and condensation rates of droplets can be obtained.

MDRs in a dielectric sphere have been studied extensively for both plane-wave illumination and Gaussian beam illumination. They exhibit themselves in the form of sharp spikelike features in the plots of various scattering characteristics versus size parameter. Recalling the MDR labeling convention, one resonance excited in a homogeneous sphere can be identified by its state of polarization and by three so-called quantum numbers l, n, and m. The mode order l is associated with the radial function and indicates the number of intensity peaks in the radial distribution of the field inside of the sphere. The mode number n is one of the classical quantization numbers for the angular momentum, which coincides with half the number of intensity maxima along the perimeter of the sphere. For a perfect sphere, there is no particular quantization axis, which leads to the fact that the resonance frequencies do not depend on mode m, therefore corresponding to a degeneracy in m for the resonances. Nevertheless, the degeneracy in m

mode can be lifted by a nonconcentric perturbation inside of the scatterer [6–9] or by a deformation in the outer surface of the particle [10–12].

The present study is more particularly devoted to the analysis of the influence of a perturbation inside the particle on MDR properties. More specifically, the scattering model of a sphere with an eccentrically located spherical inclusion is studied in this paper, a geometry that has also been analyzed by several groups. Indeed, as we know, the analysis of MDR properties has attracted much attention particularly because the MDRs can significantly enhance internal field intensities with ultrahigh quality factors (Qs) of MDRs that can reach 10^8, enabling nonlinear optical processes such as fluorescence, stimulated Raman scattering (SRS), and stimulated Brillouin scattering (SBS) to occur in droplets with a relatively low level of pumping power. Nevertheless, such high Qs of MDRs can be greatly influenced by nonconcentric perturbation inside of the droplet. Numerous interesting observations, such as spectral line broadening and laser emission, have been reported. In the analysis of resonance locations and Qs of MDRs in an inhomogeneous sphere with a small perturbation in refractive index carried out by Mazumder *et al.* [13], an increase in the refractive index in a nonconcentric spherical region inside the larger sphere leading to a decrease of resonance frequencies was reported. Fuller [14] discovered that a spectral shift of the resonance peak might be brought up when the inclusion is located in the forward hot spot of the host sphere. Furthermore, predicted by Leung *et al.* [8], MDRs in a dielectric sphere with many tiny inclusions may split into multiplets because of the loss of spherical symmetry and manifest themselves as broadened spectral lines in the scattering cross section. Similar results were also presented by Rao *et al.* [9] in considering a system of an inclusion sphere embedded in a larger sphere.

Because of the fact that all of the previous theoretical analysis of MDR behaviors in a host sphere containing an eccentric spherical inclusion (in short, an eccentric sphere, with variants) was carried out in the case of plane-wave illumination, our motivation in this paper is to study the properties of MDRs excited in an eccentric sphere with illumination by a tightly focused Gaussian beam. This scattering model under study is of great interest because, when the inclusion inside of the host sphere approaches the rim of the host sphere, then, on one hand, some MDRs may be suppressed or even annihilated by the embedded inclusion resulting in a loss of the high Qs, which may block the phenomena of SRS, SBS, and so on. But, on the other hand, some MDRs might be extensively enhanced due to the complex optical interaction between the spherical inclusion and the host sphere, which form a dielectric annular billiard, which can possibly be used as a quantum chaotic model of a micro-optical resonator [15,16]. Under favorable circumstances, these highly enhanced MDRs can be manipulated to realize an efficient coupling to the external medium in a specific orientation, leading to potential practical applications in novel light transition devices, compact laser cavities, high-sensitivity biosensors as well as microparticle characteristics [17,18].

Within the framework of the generalized Lorenz–Mie theory (GLMT), the scattering problem of an eccentric sphere illuminated by an arbitrary shaped beam was originally studied by Gouesbet and Gréhan [19], however, only in a formal way, without any numerical results. Numerical results for far-zone field distribution were given later by Han *et al.* [20] and Yan *et al.* [21]. By virtue of the recent theoretical results in the GLMT concerning the description of an arbitrary shaped beam in an arbitrary orientation [22–26], numerical results for spatial distributions of external and internal fields under off-resonance conditions have been recently presented [27]. In the present paper, the properties of MDRs excited in an eccentric sphere under illumination by tightly focused beams are studied. Corresponding results for plane-wave illumination are also presented for the sake of comparison. These calculations will provide insights for the understanding of previously reported experimental observations as well as providing guidelines for future experiments in biological observation and particle characterization.

The body of the present paper is organized as follows. In Section 2, we briefly present a theoretical treatment for the scattering problem of an eccentric sphere illuminated by an arbitrary shaped electromagnetic beam in an arbitrary orientation in the framework of the GLMT. In Section 3, a tightly focused Gaussian beam in the fundamental mode (TEM_{00}) is specifically considered for numerical illustration. The behaviors of MDRs excited in an ethanol sphere with a glass inclusion are analyzed under parallel and oblique illuminations of an off-axis Gaussian beam. Some results and discussions are summarized in Section 4, which also serves as a conclusion.

2. THEORETICAL ANALYSIS BY THE GLMT

A. Definition of the Problem

The geometry of the specific scattering problem under study is illustrated in Fig. 1. The host sphere is attached to a global Cartesian coordinate system $(O_1X_1Y_1Z_1)$, and its corresponding spherical coordinates are designated as $(r_1, \theta_1, \varphi_1)$. A spherical inclusion is embedded in the host sphere. It is attached to an inclusion coordinate system $(O_2X_2Y_2Z_2)$ whose corresponding spherical coordinates are designated as $(r_2, \theta_2, \varphi_2)$. The three axes in the inclusion coordinate

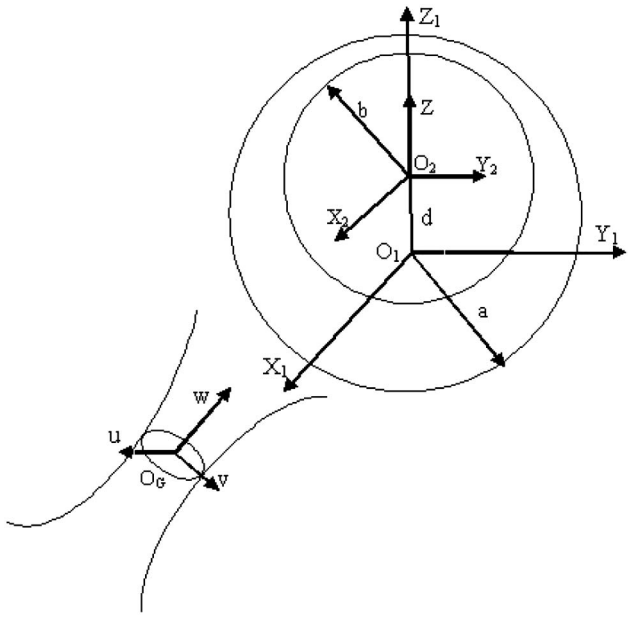

Fig. 1. Scattering geometry of the problem under study.

system are parallel to the corresponding axes in the global coordinate system, respectively.

Without any loss of generality, the center of the inclusion is located on the z axis of the global coordinate system. The center–center separation distance being designated by d, we have

$$x_2 = x_1, \qquad y_2 = y_1, \qquad z_2 = z_1 - d. \tag{1}$$

The radii of the host sphere and of the inclusion are a and b, respectively. The complex refractive index and wavenumber of the surrounding medium are m_0 and k_0, respectively. The corresponding parameters for the host sphere are m_1 and k_1 and for the inclusion m_2 and k_2.

The scattering model in Fig. 1 is illuminated by an arbitrary shaped beam propagating along the w axis in the beam coordinate system $OgUVW$. The coordinates of its origin Og with respect to the global coordinate system $(O_1X_1Y_1Z_1)$ are denoted as (x_0, y_0, z_0). The frame system $(O_1X_1Y_1Z_1)$ can be obtained from the beam coordinate system (O_gUVW) by rotations through Euler angles (α, β, γ) [22–26] followed by a translation of (x_0, y_0, z_0) and vice versa. The time-dependence factor reading as $\exp(jwt)$ is assumed, where w is the angular frequency. This term will be omitted from all formulae for the sake of conciseness.

B. Solutions

As already mentioned, the theoretical treatment to the scattering of a sphere with an eccentrically located spherical inclusion illuminated by an arbitrary shaped beam was originally presented by Gouesbet and Gréhan [19]. Afterward, Han *et al.* [20] and Yan *et al.* [21] also studied this problem and analyzed the scattered field in the far zone. Both the external field and internal field intensity distributions at off-resonance conditions were very recently presented by Wang *et al.* [27]. Therefore, we will not focus on these derivations but only recall some expressions useful for the sequel.

In the global coordinate system, an arbitrary shaped beam in an arbitrary orientation illuminating the host sphere may be expressed in terms of vector spherical wave functions (VSWFs) with two sets of expansion coefficients a_{nm} and b_{nm} according to

$$\mathbf{E}^{\text{inc}} = \sum_{n=1}^{\infty} \sum_{m=-n}^{+n} a_{nm}\mathbf{M}_{nm}^{(1)}(k_0\mathbf{r}_1) + b_{nm}\mathbf{N}_{nm}^{(1)}(k_0\mathbf{r}_1), \tag{2}$$

in which the field strength E_0 has been set equal to unity. Furthermore, the relationship between the expansion coefficients a_{nm}, b_{nm} on one hand and the more traditional beam shape coefficients $g_{n,X}^{m}$ on the other hand is available from [28] and will be provided in the sequel.

Similarly, the scattered field may be expanded using the spherical Bessel functions of the fourth kind (in the VSWFs):

$$\mathbf{E}^{\text{sca}} = \sum_{n=1}^{\infty} \sum_{m=-n}^{+n} c_{nm}\mathbf{M}_{nm}^{(4)}(k_0\mathbf{r}_1) + d_{nm}\mathbf{N}_{nm}^{(4)}(k_0\mathbf{r}_1). \tag{3}$$

The main field in the annular zone between the surface of the host sphere and that of the inclusion may be expressed using the spherical Bessel functions of the third and the fourth kind in the global coordinates system, indicating a superposition of incoming and outcoming partial waves:

$$\mathbf{E}^{\text{int1}} = \sum_{n=1}^{\infty} \sum_{m=-n}^{+n} e_{nm}\mathbf{M}_{nm}^{(3)}(k_1\mathbf{r}_1) + f_{nm}\mathbf{N}_{nm}^{(3)}(k_1\mathbf{r}_1) + v_{nm}\mathbf{M}_{nm}^{(4)}(k_1\mathbf{r}_1) + h_{nm}\mathbf{N}_{nm}^{(4)}(k_1\mathbf{r}_1). \tag{4}$$

In the inclusion coordinate system, the main field can be expanded as

$$\mathbf{E}^{\text{int1}} = \sum_{n=1}^{\infty} \sum_{m=-n}^{+n} r_{nm}\mathbf{M}_{nm}^{(3)}(k_1\mathbf{r}_2) + s_{nm}\mathbf{N}_{nm}^{(3)}(k_1\mathbf{r}_2) + t_{nm}\mathbf{M}_{nm}^{(4)}(k_1\mathbf{r}_2) + u_{nm}\mathbf{N}_{nm}^{(4)}(k_1\mathbf{r}_2), \tag{5}$$

and the internal field inside the inclusion can be represented as

$$\mathbf{E}^{\text{int2}} = \sum_{n=1}^{\infty} \sum_{m=-n}^{+n} p_{nm}\mathbf{M}_{nm}^{(1)}(k_2\mathbf{r}_2) + q_{nm}\mathbf{N}_{nm}^{(1)}(k_2\mathbf{r}_2). \tag{6}$$

In order to obtain the solutions to the scattering problem, the expansion coefficients of the fields can be related by application of the boundary conditions at the sphere surface $r_1 = a$ and at the inclusion surface $r_2 = b$. It is worth noticing that the VSWFs in the global coordinate system in Eq. (4) and those in the inclusion coordinate system Eq. (5) are different and they can be related by applying translational addition theorems of VSWFs; please refer to [19,27] for more details.

The extinction cross sections can be obtained by a similar procedure as for a spherical particle [29], but they are given as

$$C_{\text{ext}} = \frac{\lambda^2}{\pi}\text{Re}\left[\sum_{n=1}^{\infty} \sum_{m=-n}^{+n} \frac{2n+1}{n(n+1)} \frac{n+|m|!}{n-|m|!} \times (c_{nm}a_{nm}^{*} + d_{nm}b_{nm}^{*})\right]. \tag{7}$$

The normalized differential scattering cross section is given by

$$\sigma_{\text{sca}} = \frac{|\mathbf{E}^{\text{sca}}|^2}{\pi a^2}. \tag{8}$$

C. Beam Shape Coefficients for an Arbitrary Shaped Beam in an Arbitrary Orientation

In the GLMT, the electromagnetic components of the illuminating beam are described by multipole expansions over a set of basis functions. The expansion coefficients are expressed versus fundamental coefficients, usually denoted as $g_{n,X}^{m}$ [X is transverse electric (TE) or transverse magnetic (TM), with n from 1 to ∞, m from $-n$ to n], known as beam shape coefficients (BSCs). These BSCs are used to express electromagnetic fields of laser beams in expanded forms, for use in GLMTs, or in other light scattering approaches, such as the extended boundary condition method. Their calculations form the key issue, and the most difficult one, when dealing with a GLMT. Initiated by Han *et al.* [30,31], a systematic analysis was made recently concerning the transformation of BSCs through rotations of coordinate systems, and corresponding results are published in a series of papers [22–26], providing us with

a new tool for further studies, especially in cases of nonspherical or composite scatterers.

The relationships between the expansion coefficients a_{nm}, b_{nm} on one hand and the BSCs $\tilde{g}^m_{n,X}$ on the other hand read as [22]

$$a_{nm} = -ikc_n^{pw}(-1)^m(-1)^{\frac{m-|m|}{2}}\frac{(n-m)!}{(n-|m|)!}\frac{\tilde{g}^m_{n,\mathrm{TE}}}{c_n^m}, \tag{9}$$

$$b_{nm} = kc_n^{pw}(-1)^m(-1)^{\frac{m-|m|}{2}}\frac{(n-m)!}{(n-|m|)!}\frac{\tilde{g}^m_{n,\mathrm{TM}}}{c_n^m}, \tag{10}$$

in which c_n^{pw} are plane-wave coefficients reading as [29]

$$c_n^{pw} = \frac{1}{k}(-i)^{n+1}\frac{2n+1}{n(n+1)}. \tag{11}$$

According to the transformation theorem for BSCs in spherical coordinates [22], the tilde-decorated BSCs $\tilde{g}^m_{n,X}$ in a rotated system are expressed versus the BSCs $g^m_{n,X}$ in another system, called the unrotated system, as

$$\tilde{g}^m_{n,X} = \mu_{nm}\sum_{s=-n}^{n}\frac{H^m_{sn}}{\mu_{ns}}g^s_{n,X}, \tag{12}$$

where

$$\mu_{nm} = (-1)^m(-1)^{\frac{m-|m|}{2}}\frac{(n-|m|)!}{(n-m)!}, \tag{13}$$

$$H^m_{sn} = (-1)^{n+s}\frac{(n-m)!}{(n-s)!}e^{im\gamma}e^{is\alpha}\sum_{\sigma}(-1)^{\sigma}\binom{n+s}{n-m-\sigma}\binom{n-s}{\sigma} \times\left(\cos\frac{\beta}{2}\right)^{2\sigma+m+s}\left(\sin\frac{\beta}{2}\right)^{2n-2\sigma-m-s}, \tag{14}$$

in which (α,β,γ) are Euler angles bringing the unrotated system to the rotated system, whose definitions could be found in [22–26].

With decades of effort devoted to the description of an arbitrary shaped beam, the BSCs of an arbitrary shaped beam in the unrotated coordinate system $g^m_{n,X}$ can be evaluated by several methods, sharing various degrees of time running efficiency, or of flexibility, which are described in detail in a very recent book with computation programs by Gouesbet and Gréhan [32]. In our computer program, the modified localized approximation method [33], which was rigorously justified by Gouesbet and Lock [34,35], is applied to evaluate the BSCs in the unrotated coordinate system due to the fact that it provides the most efficient method, with regard to computational time, by orders of magnitude with respect to other methods such as by using quadratures [36]. It is also the most appealing from a physical point of view because it provides many physical insights on the interpretation of beam models [37].

3. NUMERICAL RESULTS AND DISCUSSIONS

MDRs will exhibit themselves in the form of supernarrow spikelike features in the plots of various scattering characteristics versus size parameter, such as extinction efficiency spectra. They can also be observed in scattered intensity spectra at a specific orientation. Actually, the resonances become in general more pronounced with increasing scattering angles since the scattered intensity is greatly reduced in the backscattering direction. Nevertheless, it is worthy to mention that some of the resonances can vanish at the scattering angle of 90° because the associated Legendre functions are equal to zero for certain modes n [38].

In this section, simulations concerning the MDRs excited by a focused Gaussian beam or a plane wave are made by using a homemade code [27] within the framework of the GLMT. The correctness of the code has already been checked in several ways, including by comparing results with those obtained from a widely used code published by Ngo *et al.* [39] and with published research data [20,40].

Exemplifying results about extinction efficiency spectra and normalized differential scattering cross sections in a specific direction are displayed in the following. Because of the fact that the normalized differential scattering cross sections calculated by using Eq. (8) are proportional to the intensity, it is conveniently referred to as intensity in the present paper. The case of a focused fundamental Gaussian beam (TEM_{00} mode) illuminating an ethanol sphere (having a real refractive index equal to 1.36) with an eccentrically located spherical glass inclusion (having a real refractive index equal to 1.50) is simulated. This model can be regarded as a glass bead covered inhomogeneously with an ethanol coating illuminated by a laser beam. The wavelength of the laser beam is assumed to be $\lambda = 0.532\,\mu$m, and the beam waist radius is $w_0 = 1.0\,\mu$m. Furthermore, a plane wave can be obtained by setting w_0 to be much larger than the radius of the host sphere, say, $w_0 = 100R$. The amplitude of the beam at its focal point is set to be unity without any loss of generality.

A. Parallel Illumination by an Off-Axis Gaussian Beam

Previous observations [41] in experiments and results in numerical calculations of the light scattered by a homogeneous sphere or a concentric sphere illuminated by a Gaussian beam show that the excitation of MDRs depends significantly on the focal center position and the polarization of the incident beam [40,42,43]. As the beam is shifted farther away from the particle center, the fraction of the incident energy coupled into the sphere at resonance first increases and then decreases [40]. Electromagnetic energy is most efficiently coupled into MDRs when a laser beam is focused near the edge of a particle. Results in our simulations also support these mentioned conclusions. Thus, for exemplifying results, an off-axis Gaussian beam, which is aligned at the edge of the scatterer, is applied as an excitation source to excite MDRs. The Gaussian beam is assumed to propagate in the z-axis direction with its electric vector polarized along the x axis at its waist center. The focal center of the Gaussian beam is shifted along the x axis to a constant distance $a = 2.93357\,\mu$m relative to the center of the droplet, which corresponds to the radius of an ethanol sphere when the $\mathrm{TE}_{41,1}$ ($n = 41$, $l = 1$) resonance is excited.

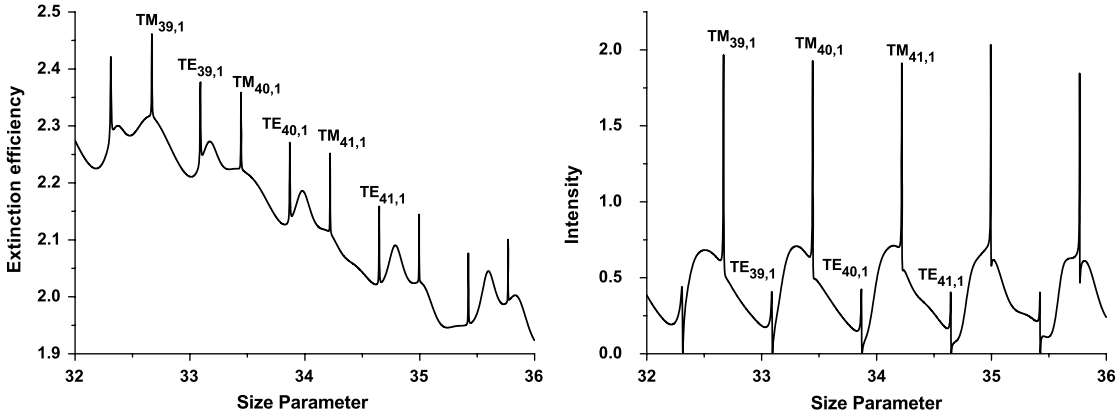

(a) Extinction efficiency spectrum (b) Backward intensity spectrum

Fig. 2. Extinction efficiency spectrum and backward intensity spectrum for a concentric sphere. The radius of the inclusion is $r = 0.7R$, plane-wave illumination with incidence angle 0.0°.

With plane-wave illumination, extinction efficiency and scattered intensity at scattering angle 180° are shown in Fig. 2 for a concentric sphere as a function of size parameter. The radius of the host sphere is denoted by R, and the radius of the inclusion is specified as a ratio of the host sphere radius $r = 0.7R$. Both TE and TM resonances are visible in Fig. 2. It is obvious that the resonances in the backscattering direction [Fig. 2(b)] are much more pronounced than those in the extinction efficiency spectrum [Fig. 2(a)].

With Gaussian beam illumination, comparisons of extinction efficiency and of scattered intensity at scattering angle 180° as a function of size parameter are shown in Fig. 3 for a concentric sphere and an eccentric sphere. The radius of the inclusion is $r = 0.7R$. The displacement of the inclusion with respect to the host sphere center is designated as a center–center separation distance $d = 0.1R$ for the eccentric sphere. In Fig. 3, both the first-order ($l = 1$) and the second-order ($l = 2$) resonances are clearly visible. Compared with plane-wave illumination, only TE resonances can be seen in Fig. 3 with Gaussian beam illumination. A similar calculation shows that only TM resonances can be seen if the Gaussian beam shifts along the y axis instead of along the x axis. This is agreement with the fact that only tangential components of the electromagnetic field can be sufficiently coupled into the resonances. For a concentric sphere or a multilayered sphere, the scattered field coefficients with an illumination of arbitrary shaped beam in the framework of the GLMT are actually proportional to the corresponding scattered field coefficients with a plane-wave illumination in the Lorenz–Mie theory (LMT) [44]; thus, the MDRs found in Fig. 3 for the concentric sphere are located at the same positions as those in Fig. 2.

As we can see from Fig. 2, especially from Fig. 2(b), the amplitudes of the first-order resonance peaks $l = 1$ are not changed a lot under a plane-wave illumination in the limited size parameter range shown in Fig. 2. Nevertheless, the amplitudes of the first-order resonance peaks decrease monotonically under the focused Gaussian beam illumination, which can be observed in Fig. 3, particularly in Fig. 3(b). This can be explained by invoking the localization principle [37,45], according to which the nth partial wave is associated with a bunch of rays passing through a radial position $(n + 1/2)(\lambda/2\pi)$ from the scatterer center, where λ is the wavelength. Thus, only certain resonances can be strongly excited by a focused laser beam depending greatly on the shape pattern as well as on the focal center location of the laser beam. For the simulations in this paper, the focal center of the Gaussian beam is shifted along the x axis with $a = 2.93357\,\mu$m, which corresponds to the $TE_{41,1}$ resonance, so that resonances modes around $n = 41$ are more pronounced. It is interesting to find that the most enhanced resonances are

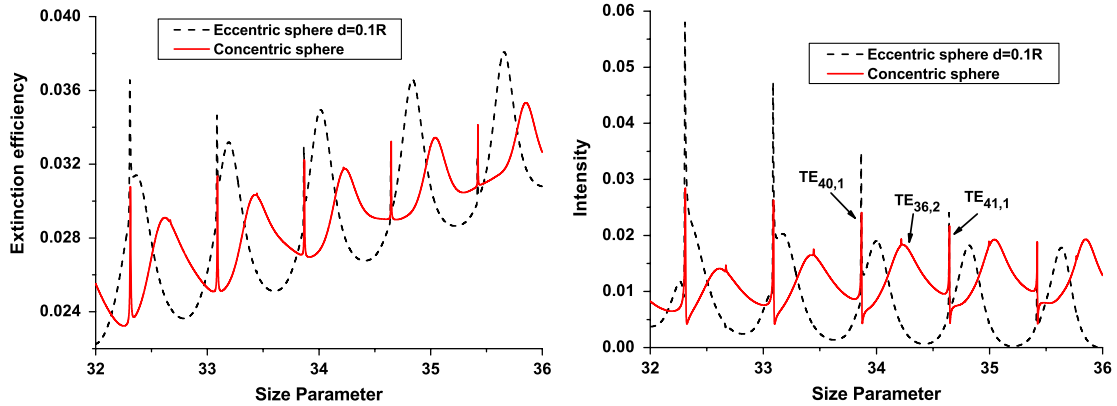

(a) Extinction efficiency spectrum (b) Backward intensity spectrum

Fig. 3. (Color online) Comparison of extinction efficiency spectra and of backward intensity spectra for a concentric sphere and an eccentric sphere ($d = 0.1R$), respectively. The radius of the inclusion is $r = 0.7R$, Gaussian beam illumination with incidence angle 0.0°.

for the modes a little bit smaller than $n = 41$. This is agreement with the result that the fraction of the internal energy is most efficiently coupled to the resonances when the focused beam center is located slightly outside of the particle [40].

Compared with the concentric sphere, the second-order resonances ($l = 2$) in the eccentric sphere with a separation distance $d = 0.1R$ are greatly affected by the shift of the inclusion. Nevertheless, the first-order resonances ($l = 1$) are little affected. This is reasonable because, for an inclusion with $r = 0.7R$, a small displacement of the inclusion $d = 0.1R$ cannot affect the first-order resonances efficiently because they are closer to the rim of the particle. As has been mentioned above, each resonance in a sphere or a concentric sphere can be identified by its state of polarization and two quantum numbers n, l and does not depend on mode m, such as the label $TE_{41,1}$ indicates the resonance is predominantly in the c_{nm} coefficients at quantum numbers $n = 41, l = 1$. Nevertheless, the resonances in an eccentric sphere cannot be labeled like this. This is due to the fact that each resonance in the eccentric sphere is contributed by several n modes instead of a single n mode, which was also mentioned by Rao *et al.* [9]. Thus, all the resonances in an eccentric sphere are not labeled in the figures of this paper.

Heated by the laser beam or by any possible heating method, such as by putting it close to a hot iron wall, the ethanol coating would become thinner because of evaporation. Accordingly, in Fig. 4, the radius of the inclusion is specified as $r = 0.92R$ to indicate a very thin film of ethanol coating. A center–center separation distance $d = 0.04R$ is assumed. The other parameters are exactly the same than the ones used in Fig. 3. Compared with the case when $r = 0.7R$ with $d = 0.1R$, the positions of the first-order resonances shift much more in Fig. 4 when $r = 0.92R$, even with a smaller displacement of the inclusion $d = 0.04R$. Similar to the behavior in Fig. 3, the second-order resonances in Fig. 4 are also much more affected than the first-order resonances. This is because more energy from the second-order modes overlap with the core region. It is interesting to find that the amplitudes of the first-order resonances decrease a lot in the eccentric sphere with $d = 0.04R$ compared to that in the concentric sphere, which may be due to the fact that the electromagnetic energy at the first-order resonances is more efficiently coupled into the inclusion in the eccentric sphere than in the concentric sphere.

Furthermore, with Gaussian beam illumination, extinction efficiency and backscatter intensity are plotted in Fig. 5 as a function of size parameter for a concentric sphere of $r = 0.7R$ and for a concentric sphere of $r = 0.92R$. It is obvious that, as the relative radius of the inclusion with respect to the host sphere increases, both the first-order and second-order resonances shift dramatically. And the second-order resonances are significantly enhanced.

B. Oblique Illumination by an Off-Axis Gaussian Beam

As reported by Rao *et al.* [9], with a parallel illumination by a plane wave, that is to say, when the wave travels along the z axis in our case, which indicates the incidence angle is zero, the degeneracy in mode m is not lifted for an eccentric sphere. This is reasonable because the symmetry of the scatterer is not broken in the azimuthal direction with regard to the incident direction of plane wave. Indeed, we have shown in Subsection 3.A that the degeneracy in mode m is also not lifted with a parallel illumination by an off-axis Gaussian beam.

In the following calculations, the incidence angle of the Gaussian beam is assumed to be 90°, in which case the asymmetry of an eccentric sphere reaches the largest extent for a fixed center–center separation distance d. More specifically, the Gaussian beam is assumed to propagate in the x-axis direction with its electric vector polarized in the z axis at its waist center. The focal center of the Gaussian beam is situated on the z axis with a constant distance $z_0 = 2.93357\,\mu$m.

With a plane-wave illumination, as we can see from Fig. 6, splitting in MDRs are observed for modes having sufficiently high Qs. More detailed information for single resonance peaks can be obtained in the insets. It shows that the TM resonance peaks are more easily lifted than the TE resonance peaks.

With a tightly focused Gaussian beam illumination, extinction efficiency as a function of size parameter for an eccentric sphere of $r = 0.7R$ with different displacements of the inclusion is shown in Fig. 7, and that for an eccentric sphere of $r = 0.92R$ with different displacements of the inclusion is shown in Fig. 8. In contrast with the case of a plane-wave illumination, splitting in resonance peaks are not observed in the extinction efficiency spectrum for the focused Gaussian beam illumination. For the eccentric sphere with $r = 0.7R$ in Fig. 7,

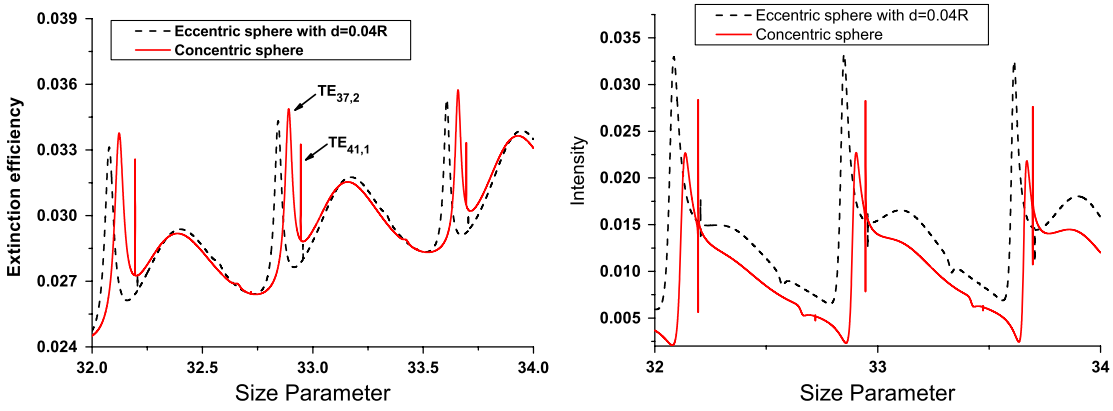

(a) Extinction efficiency spectrum (b) Backward intensity spectrum

Fig. 4. (Color online) Comparison of extinction efficiency spectra and of backward intensity spectra for a concentric sphere and an eccentric sphere ($d = 0.04R$), respectively. The radius of the inclusion is $r = 0.92R$, Gaussian beam illumination with incidence angle 0.0°.

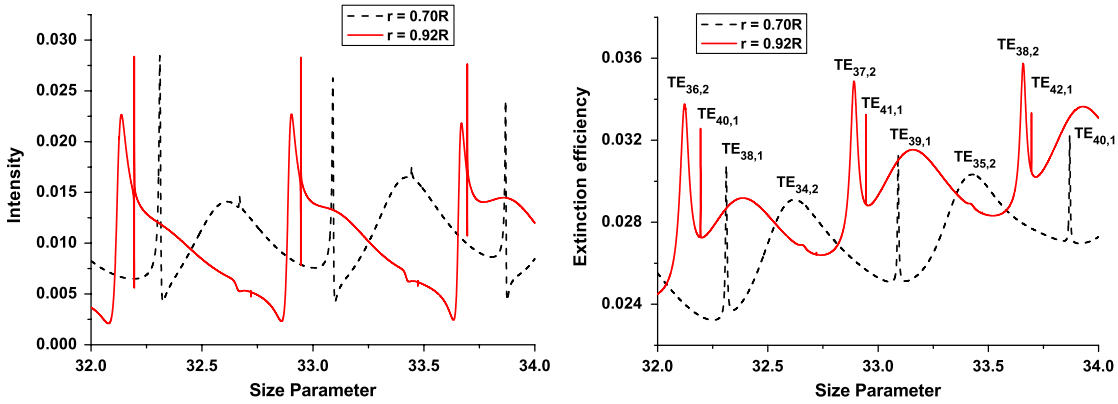

(a) Extinction efficiency spectrum (b) Backward intensity spectrum

Fig. 5. (Color online) Comparison of extinction efficiency spectra and of backward intensity spectra for concentric spheres of $r = 0.7R$ and of $r = 0.92R$, respectively. Gaussian beam illumination with incidence angle 0.0°.

the effects on the second-order resonances due to the eccentric shift of inclusion are very significant, while there is much less influence on its first-order resonances. For the eccentric sphere with $r = 0.92R$ in Fig. 8, all the amplitudes of first-order and second-order resonances are enhanced step by step as the inclusion approaches the symmetric axis of the Gaussian beam from $d = -0.04R$ to $d = 0.0$ and then to $d = +0.04R$. It is interesting to find that the first-order resonances are greatly suppressed for $d = -0.04R$ while the first-order resonances are greatly enhanced for $d = +0.04R$.

Furthermore, as for spheres or concentrically multilayered spheres [44], the scattered field coefficients for eccentric spheres with an illumination of arbitrary shaped beam in the framework of the GLMT are also proportional to the corresponding scattered field coefficients with a plane-wave illumination; thus, the MDRs found in Fig. 6 for the eccentric sphere are located at the same positions as those in Fig. 8.

C. Internal Field Distribution

In contrast with the behaviors of MDRs with a plane-wave illumination, splittings in the resonance peaks are not observed in the extinction efficiency spectrum with a tightly focused Gaussian beam illumination. To provide additional information with regard to the pattern of the MDRs, plots of internal field distributions for some resonances are presented.

Even though the magnitude and the phase for each partial wave component of the electromagnetic field can be determined from the GLMT formalism, a useful visualization of the field distribution can be obtained by plotting the normalized source function as a function of spatial position. The normalized source function is defined as

$$S = |\mathbf{E}|^2/|E_0|^2, \tag{15}$$

where $\mathbf{E}$ is the electric vector of the internal or external field and E_0 is the electric field strength of the incident field, which is assumed to be unity. To emphasize the internal distribution, the external field intensities are suppressed to zero in the

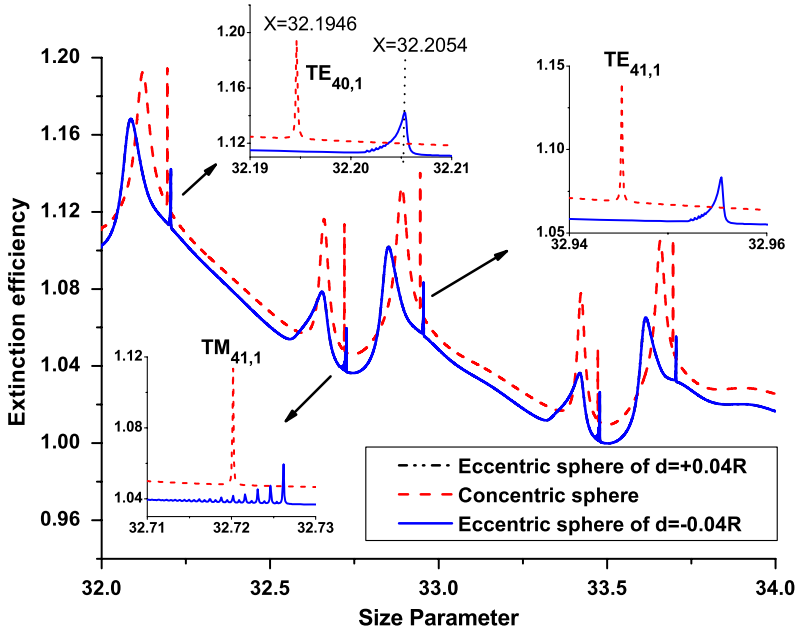

Fig. 6. (Color online) Comparison of extinction efficiency spectra for a concentric sphere and eccentric spheres ($d = 0.04R$, $d = -0.04R$). The radius of the inclusion is $r = 0.92R$, plane-wave illumination with incidence angle 90.0°.

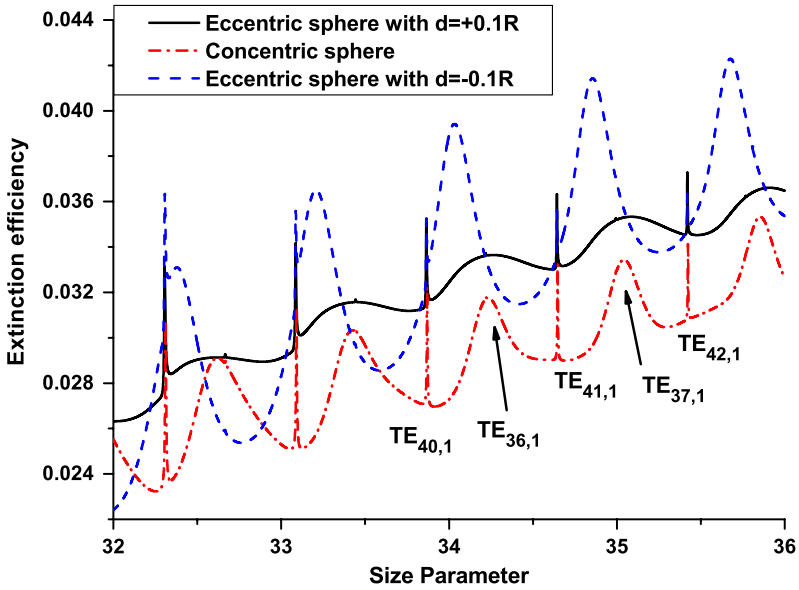

Fig. 7. (Color online) Comparison of extinction efficiency spectra for eccentric spheres of $r = 0.7R$ with different center–center separation distances illuminated by a Gaussian beam.

subsequent figures, and the spatial coordinates are normalized by the host sphere radius.

Calculations of internal field distribution for an off-resonance case, a complete resonance case in a concentric sphere, and a broken-resonance case in an eccentric sphere are shown in Figs. 9(a)–9(c), respectively, for a plane-wave illumination and in Figs. 9(d)–9(f), respectively, for a tightly focused Gaussian beam illumination. Parameters used in Figs. 9(a)–9(c) are the same as the ones used in Fig. 6, and parameters used in Figs. 9(d)–9(f) are the same as the ones used in Fig. 8.

For a plane-wave illumination, a picture of an off-resonance case at size parameter $x = 32.19$ for the eccentric sphere is plotted in the transverse x–z plane in Fig. 9(a). Figure 9(b) is the $TE_{40,1}$ resonance occurring in the concentric sphere at size parameter $x = 32.1946$. The largest enhancements are near the forward- and backward-scattering directions. Detailed study of the resonance reveals that the $TE_{n,1}$ mode resonance has n peaks in each side of the x–z plane with the z axis as a symmetric axis. Nevertheless, this symmetry is broken if the inclusion is shifted eccentrically to the rim of the host sphere. Figure 9(c) shows the internal field distribution of a broken resonance at size parameter $x = 32.2054$. The largest enhancements are found to be shifted away from the forward- and backward-scattering directions. The intensity peaks around the rim of the sphere become blurred because several m modes contribute to the resonance.

For a tightly focused Gaussian beam illumination, Fig. 9(d) is a plot of internal field distribution for an eccentric sphere with $d = -0.04R$ at off-resonance with size parameter $x = 32.19$. Figure 9(e) shows the $TE_{40,1}$ resonance occurring in an concentric sphere with size parameter $x = 32.1946$. A

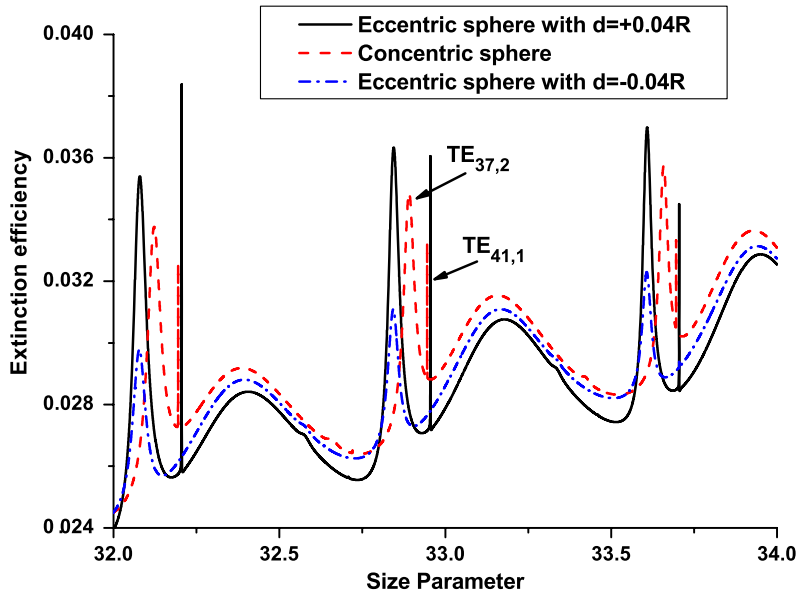

Fig. 8. (Color online) Comparison of extinction efficiency spectra for eccentric spheres of $r = 0.92R$ with different center–center separation distances illuminated by a Gaussian beam.

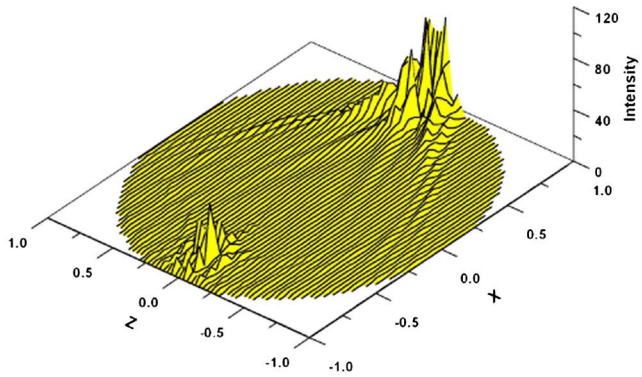

(a) Off-resonance case at $x = 32.19$

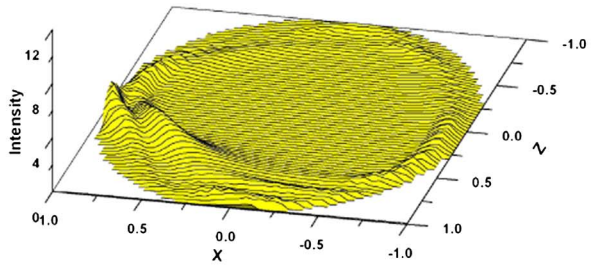

(d) Off-resonance case at $x = 32.19$

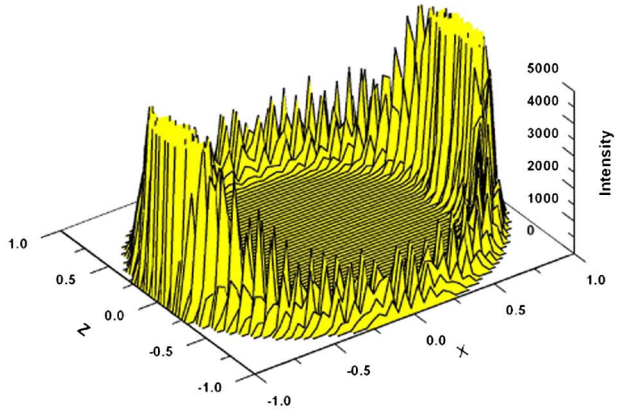

(b) Complete resonance case at $x = 32.1946$

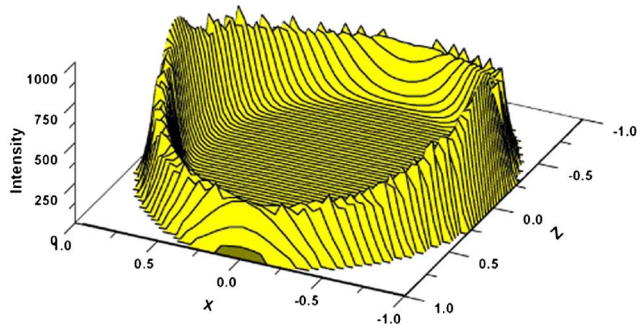

(e) Complete resonance case at $x = 32.1946$

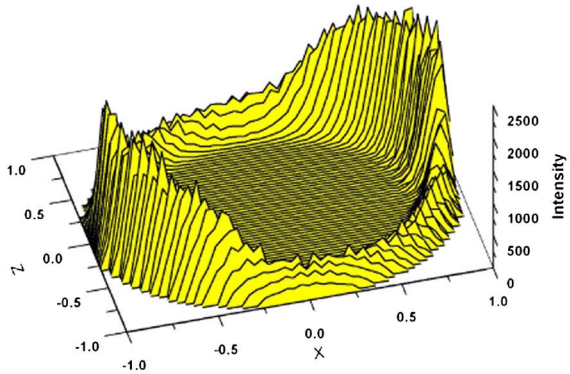

(c) Broken resonance case at $x = 32.2054$

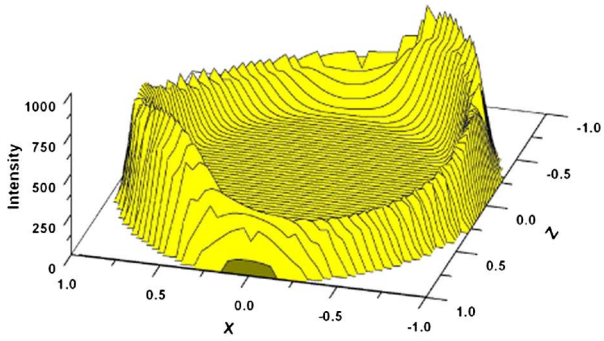

(f) Broken resonance case at $x = 32.2054$

Fig. 9. (Color online) Distributions of internal field for an eccentric sphere illuminated by (a), (b), (c) plane wave and (d), (e), (f) Gaussian beam. (a), (d) off-resonance case with $d = -0.04R$; (b), (e) complete resonance case with $d = 0.0R$, and (c), (f) broken-resonance case with $d = 0.04R$. The radius of the inclusion is $r = 0.92R$. The incident wave propagates along the x axis from negative to positive.

broken-resonance case occurring in an eccentric sphere with size parameter $x = 32.2054$ is presented in Fig. 9(f). For the on-resonance cases in Figs. 9(e) and 9(f), enhancements in the internal intensity are excited near the edge of the host sphere. Different from the pattern of separated peaks observed for the plane-wave illumination in Figs. 9(b) and 9(c), a solid ring formation is displayed for the Gaussian beam illumination. For a concentric sphere, a symmetric formation of the resonance is obtained with greatest field intensities near the forward- and backward-scattering directions. For an eccentric sphere, although the degeneracy of the mode m is not observed in the extinction efficiency spectra, the symmetric formation of the internal field distribution at resonance conditions becomes asymmetric with largest field intensity locations shifted away from the forward- and backward-scattering directions.

4. CONCLUSIONS AND DISCUSSION

Following the recent results in the GLMT concerning the description of an arbitrary shaped beam in an arbitrary orientation [22–27], the properties of MDRs excited in an

ethanol sphere (having a real refractive index equal to 1.36) with an eccentrically located spherical glass inclusion (having a real refractive index equal to 1.50) illuminated by a tightly focused Gaussian beam is studied. Corresponding calculations for plane-wave illumination are also made for the sake of comparison.

As for spheres and concentrically multilayered spheres, since the scattered field coefficients with an illumination by arbitrary shaped beam in the framework of the GLMT are proportional to the corresponding scattered field coefficients with a plane-wave illumination in the LMT, the resonance positions of MDRs in eccentrically layered spheres are equal for laser beam illumination and for plane-wave illumination. With an illumination of a tightly focused Gaussian beam, the positions and the amplitudes of the MDRs peaks excited in an eccentric sphere depend greatly on the relative size of the inclusion with respect to the host sphere and on the separation distance between the two sphere centers. The amplitudes of the MDR peaks are also found to be very sensitive to the relative location and the polarization status of the laser beam. In the simulation of a glass bead covered inhomogeneously with a very thin film of ethanol coating ($r = 0.92R$) illuminated by a Gaussian beam focused at the edge of the particle ($x = 2.93357\,\mu$m), all the first-order ($l = 1$) and second-order ($l = 2$) resonances are found to be enhanced step by step as the inclusion approaches the symmetric axis of the Gaussian beam from $d = -0.04R$ to $d = 0.0$ and then to $d = +0.04R$. It is interesting to find that the first-order resonances are suppressed for $d = -0.04R$ while the first-order resonances are greatly enhanced for $d = +0.04R$ under the tightly focused Gaussian beam illumination. Nevertheless, the extinction efficiency spectra for $d = -0.04R$ and those for $d = +0.04R$ are identical under the plane-wave illumination.

Different from the MDRs with a plane-wave illumination, only certain resonances are strongly excited by a focused laser beam depending greatly on the shape pattern as well as on the location of the focal center of the laser beam. This is easy to understand from the point of view of the localization principle. Indeed, the nth partial wave is associated with a bunch of rays passing through a radial position $(n + 1/2)(\lambda/2\pi)$ from the scatterer center. Thus, for an off-axis illumination by a tightly focused Gaussian beam, only those modes with radial position at or close to the focal center of the Gaussian beam are strongly excited.

With a tightly focused Gaussian beam illumination, splitting of the resonance peaks in the extinction efficiency spectrum is not observed for an eccentric sphere. Looking closely at the absolute value of the BSCs $|g_n^m|$ calculated by using the localization approximation method [46], it is observed that it decreases quickly as $|m|$ increases, and $|g_n^m|$ even vanish except for $|m| = 1$ when the scatterer center is located on the beam axis. Thus the high-order m terms are expected to contribute little to scattering phenomena, and the lift of degeneracy in mode m cannot be observed. Furthermore, instead of exciting only a single angular mode m, several angular modes are excited in the case of an illumination by an off-axis Gaussian beam. Thus, in contrast with the pattern of separated peaks observed in the internal field distribution at resonance condition for a plane-wave illumination, a solid ring formation is displayed for the Gaussian beam illumination. In contrast with the symmetric formation of the internal field distribution at resonance condition for a concentric sphere, asymmetric formation with largest field intensity positions shifted away from the forward- and backward-scattering directions to sideways is observed for an eccentric sphere. It indicates that the degeneracy of m modes is lifted for an eccentric sphere with a tightly focused Gaussian beam, although splitting of the resonance peaks cannot be observed in the extinction efficiency spectra.

ACKNOWLEDGMENTS

The work presented in this paper is supported by the project "Bourses Doctorales en Alternance" between France and China. This work is also partially supported by the European program INTERREG IVa-C5: Cross-Channel Centre for Low Carbon Combustion. The authors thank the reviewers for providing several constructive comments and suggestions to the present paper.

REFERENCES

1. A. Ashkin and J. M. Dziedzic, "Observation of resonances in the radiation pressure on dielectric spheres," Phys. Rev. Lett. **38**, 1351–1354 (1977).
2. P. Chýlek, J. T. Kiehl, and M. K. W. Ko, "Optical levitation and partial-wave resonance," Phys. Rev. A **18**, 2229–2233 (1978).
3. P. Chýlek, B. Ramaswamy, A. Ashkin, and J. M. Dziedzic, "Simultaneous determination of refractive index and size of spherical dielectric particles from light scattering data," Appl. Opt. **22**, 2302–2307 (1983).
4. H.-M. Tzeng, K. F. Wall, M. B. Long, and R. K. Chang, "Evaporation and condensation rates of liquid droplets deduced from structure resonances in the fluorescence spectra," Opt. Lett. **9**, 273–275 (1984).
5. G. Chen, M. M. Mazumder, R. K. Chang, J. C. Swindal, and W. P. Acker, "Laser diagnostics for droplet characterization: application of morphology dependent resonances," Progr. Energy Combust. Sci. **22**, 163–188 (1996).
6. J. Ducastel, "Etude des résonances morphologiquement dépendantes et application à la caractérisation de microparticules en milieu diphasique," Ph.D. thesis (Institut National des Sciences Appliquées de Rouen, 2007).
7. D. Ngo and R. G. Pinnick, "Suppression of scattering resonances in inhomogeneous microdroplets," J. Opt. Soc. Am. A **11**, 1352–1359 (1994).
8. P. T. Leung, S. W. Ng, and K. M. Pang, "Morphology-dependent resonances in dielectric spheres with many tiny inclusions," Opt. Lett. **27**, 1749–1751 (2002).
9. V. S. C. M. Rao and S. D. Gupta, "Broken azimuthal degeneracy with whispering gallery modes of microspheres," J. Opt. A **7**, 279–285 (2005).
10. G. Chen, R. K. Chang, S. C. Hill, and P. W. Barber, "Frequency splitting of degenerate spherical cavity mode: stimulated Raman scattering spectrum of deformed droplets," Opt. Lett. **16**, 1269–1271 (1991).
11. M. I. Mishchenko and A. A. Lacis, "Morphology-dependent resonances of nearly spherical particles in random orientation," Appl. Opt. **42**, 5551–5556 (2003).
12. Y. P. Han, L. Méès, G. Gouesbet, Z. S. Wu, and G. Gréhan, "Resonant spectra of a deformed spherical microcavity," J. Opt. Soc. Am. B **23**, 1390–1397 (2006).
13. M. M. Mazumder, S. C. Hill, and P. W. Barber, "Morphology-dependent resonances in inhomogeneous spheres: comparison of the layered T-matrix method and the time-independent perturbation method," J. Opt. Soc. Am. A **9**, 1844–1853 (1992).
14. K. A. Fuller, "Morphology-dependent resonances in eccentrically stratified sphere," Opt. Lett. **19**, 1272–1274 (1994).
15. G. Gouesbet, S. Meunier-Guttin-Cluzel, and G. Gréhan, "Periodic orbits in Hamiltonian chaos of the annular billiard," Phys. Rev. E **65**, 016212 (2001).
16. M. Hentschel and K. Richter, "Quantum chaos in optical systems: the annular billiard," Phys. Rev. E **66**, 056207 (2002).

17. S. M. Spillane, T. J. Kippenberg, and K. J. Vahala, "Ultralow-threshold Raman laser using a spherical dielectric microcavity," Nature **415**, 621–623 (2002).
18. G. Gouesbet, S. Meunier-Guttin-Cluzel, and G. Gréhan, "Generalized Lorenz–Mie theory for a sphere with an eccentrically located inclusion, and optical chaos," Part. Part. Syst. Charact. **18**, 190–195 (2001).
19. G. Gouesbet and G. Gréhan, "Generalized Lorenz–Mie theory for a sphere with an eccentrically located spherical inclusion," J. Mod. Opt. **47**, 821–837 (2000).
20. G. X. Han, Y. P. Han, J. Y. Liu, and Y. Zhang, "Scattering of an eccentric sphere arbitrarily located in a shaped beam," J. Opt. Soc. Am. B **25**, 2064–2072 (2008).
21. B. Yan, X. Han, and K. F. Ren, "Scattering of a shaped beam by a spherical particle with an eccentric spherical inclusion," J. Opt. A **11**, 015705, 2009.
22. G. Gouesbet, J. J. Wang, and Y. P. Han, "Transformations of spherical beam shape coefficients in generalized Lorenz–Mie theories through rotations of coordinate systems. I. General formulation," Opt. Commun. **283**, 3218–3225 (2010).
23. J. J. Wang, G. Gouesbet, and Y. P. Han, "Transformations of spherical beam shape coefficients in generalized Lorenz–Mie theories through rotations of coordinate systems. II. Axisymmetric beams," Opt. Commun. **283**, 3226–3234 (2010).
24. G. Gouesbet, J. J. Wang, and Y. P. Han, "Transformations of spherical beam shape coefficients in generalized Lorenz–Mie theories through rotations of coordinate systems. III. Special Euler angles," Opt. Commun. **283**, 3235–3243 (2010).
25. G. Gouesbet, J. J. Wang, Y. P. Han, and G. Gréhan, "Transformations of spherical beam shape coefficients in generalized Lorenz–Mie theories through rotations of coordinate systems. IV. Plane waves," Opt. Commun. **283**, 3244–3254 (2010).
26. G. Gouesbet, J. A. Lock, J. J. Wang, and G. Gréhan, "Transformations of spherical beam shape coefficients in generalized Lorenz–Mie theories through rotations of coordinate systems. V. Localized beam models," Opt. Commun. **284**, 411–417 (2011).
27. J. J. Wang, G. Gouesbet, Y. P. Han, and G. Gréhan, "Study of scattering from a sphere with an eccentrically located spherical inclusion by generalized Lorenz–Mie theory: internal and external field distribution," J. Opt. Soc. Am. A **28**, 24–39 (2011).
28. G. Gouesbet, "T-matrix formulation and generalized Lorenz–Mie theories in spherical coordinates," Opt. Commun. **283**, 517–521 (2010).
29. G. Gouesbet, B. Maheu, and G. Gréhan, "Light scattering from a sphere arbitrarily located in a Gaussian beam, using a Bromwich formulation," J. Opt. Soc. Am. A **5**, 1427–1443 (1988).
30. Y. P. Han, H. Y. Zhang, and G. X. Han, "The expansion coefficients of arbitrary shaped beam in oblique illumination," Opt. Express **15**, 735–746 (2007).
31. Y. P. Han, Y. Zhang, H. Y. Zhang, and G. X. Han, "Scattering of typical particles by beam shape in oblique illumination," J. Quant. Spectrosc. Radiat. Transfer **110**, 1375–1381 (2009).
32. G. Gouesbet and G. Gréhan, *Generalized Lorenz–Mie Theories* (Springer, 2011).
33. G. Gouesbet, "Validity of the localized approximation for arbitrary shaped beams in the generalized Lorenz–Mie theory for spheres," J. Opt. Soc. Am. A **16**, 1641–1650 (1999).
34. J. A. Lock and G. Gouesbet, "Rigorous justification of the localized approximation to the beam-shape coefficients in generalized Lorenz–Mie theory. I. On-axis beams," J. Opt. Soc. Am. A **11**, 2503–2515 (1994).
35. G. Gouesbet and J. A. Lock, "Rigorous justification of the localized approximation to the beam-shape coefficients in generalized Lorenz–Mie theory. II. Off-axis beams," J. Opt. Soc. Am. A **11**, 2516–2525 (1994).
36. J. A. Lock, "An improved Gaussian beam scattering algorithm," Appl. Opt. **34**, 559–570 (1995).
37. G. Gouesbet, J. A. Lock, and G. Gréhan, "Generalized Lorenz–Mie theories and description of electromagnetic arbitrary shaped beams: localized approximations and localized beam models," J. Quant. Spectrosc. Radiat. Transfer **112**, 1–27 (2011).
38. P. W. Barber and S. C. Hill, *Light Scattering by Particles: Computational Methods*, Vol. 2 of Advanced Series in Applied Physics (World Scientific, 1990).
39. D. Ngo, G. Videen, and P. Chýlek, "A FORTRAN code for the scattering of EM waves by a sphere with a nonconcentric spherical inclusion," Comput. Phys. Commun. **99**, 94–112 (1996).
40. E. E. M. Khaled, S. C. Hill, and P. W. Barber, "Light scattering by a coated sphere illuminated with a Gaussian beam," Appl. Opt. **33**, 3308–3314 (1994).
41. A. Ashkin and J. M. Dziedzic, "Observation of optical resonances of dielectric spheres by light scattering," Appl. Opt. **20**, 1803–1814 (1981).
42. J. P. Barton, D. R. Alexander, and S. A. Schaub, "Internal fields of a spherical particle illuminated by a tightly focused laser beam: focal point positioning effects at resonance," J. Appl. Phys. **65**, 2900–2906 (1989).
43. E. E. M. Khaled, S. C. Hill, and P. W. Barber, "Internal electric energy in a spherical particle illuminated with a plane wave or off-axis Gaussian beam," Appl. Opt. **33**, 524–532 (1994).
44. F. Onofri, G. Gréhan, and G. Gouesbet, "Electromagnetic scattering from a multilayered sphere located in an arbitrary beam," Appl. Opt. **34**, 7113–7124 (1995).
45. H. C. van de Hulst, *Light Scattering by Small Particles* (Peter Smith, 1982).
46. G. Gouesbet, G. Gréhan, and B. Maheu, "Localized interpretation to compute all the coefficients g_n^m in the generalized Lorenz–Mie theory," J. Opt. Soc. Am. A **7**, 998–1007 (1990).